Detector Development for Proton Computed Tomography (pCT)

H. F.-W. Sadrozinski, V. Bashkirov, B. Colby, G. Coutrakon, B. Erdelyi, D. Fusi, F. Hurley, R. P. Johnson, S. Kashiguine, S. McAllister, F. Martinez-McKinney, J. Missaghian, M. Scaringella, S. Penfold, V. Rykalin, R. Schulte, K. Schubert, D. Steinberg, A. Zatserklaniy.

***Abstract*– Proton Computed Tomography (pCT) is being developed in support of proton therapy and treatment planning. The aim of pCT, to reconstruct an accurate map of the stopping power (S.P.) in a phantom and, in the future, in patients, is being pursued with a diverse list of detector systems, using the entire arsenal of tracking and energy detectors developed for High Energy Physics (HEP). The first radiographs and 3D images are being reconstructed with prototype detectors, which will be described. Most of the existing systems are being upgraded to higher proton fluxes to reduce the scanning time.**

I. Introduction

Proton Computed Tomography (pCT) has been developed since 2002, when the need for it and the requirements were presented to the 2002 IEEE NSS/MIC Symposium audience [1]. At the 2003 IEEE/MIC Symposium, a detector system was presented [2], which incorporated the basic building blocks of a pCT system, and which was eventually built and is now taking 3D data set. These early papers outline the motivation and detector challenges for pCT, which are briefly listed in Sections II. Some of the existing or planned detector systems will be reviewed in Section III. Section IV describes the calibration of the energy loss in terms of the Water Equivalent Path Length (WEPL) of the phantom. Section V contains results from 3D image reconstruction and important "lessons learned" about the operation of a prototype pCT scanner. Detector response simulations with Geant4 in support of detector development are described in Section VI, and the resulting head scanner design and experimental sensor layout in Section VII.

Manuscript received November 9, 2011.

This work was supported in part by Award Number R01EB013118 from the National Institute of Biomedical Imaging and Bioengineering (NIBIB), the US Department of Defense (DoD) and the US Army Medical Research Activities and Acquisitions.

H. F.-W. Sadrozinski is with the SCIPP, UC Santa Cruz, CA 95064, USA (telephone: 831-459-4670, e-mail:hartmut @scipp.ucsc.edu).

B. Colby, D. Fusi, R. P. Johnson, S. Kashiguine, F. Martinez-McKinney, J. Missaghian, M. Scaringella, D. Steinberg, A. Zatserklanyi, are with SCIPP, UC Santa Cruz, CA 95064, USA.

V. Bashkirov, F. Hurley, R. Schulte are with Loma Linda University Medical Center, CA 92354, USA.

G. Coutrakon, B. Erdelyi, V. Rykalin. are with Northern Illinois University DeKalb, IL 60115, USA.

S. McAllister, K. Schubert are with CSU San Bernardino, San Bernardino, CA 92407, USA.

S. Penfold is with the Centre for Medical Radiation Physics, University of Wollongong NSW 2522, Australia

II. Motivation and Challenges for PCT

Proton therapy and treatment planning requires the knowledge of the stopping power (S.P.) in the patient, such that by tuning the proton energy, the Bragg peak can be located within the tumor. At present, the stopping power is derived from X-ray CT scans by converting the linear X-ray attenuation coefficient ("Hounsfield values") to relative S.P. with respect to water. This method has been shown to accurately predicting the Bragg peak location to only 3-4% of the proton range and to be less accurate in the presence of complicated tissue-air and tissue-bone interfaces [3]. In addition, tissues with the same Hounsfield values can have different S.P. values.

The goal of Proton CT is to reconstruct a 3D map of the S.P. within the patient with as fine a voxel size as practical at a minimum dose, by a measurement of the energy loss or residual proton range.

There are several practical challenges when using protons for imaging. The first one is Multiple Coulomb Scattering (MCS). Protons passing through material are not traveling along straight lines like X-rays. The consequence is that the proton path inside the patient/phantom has to be reconstructed for every proton from the direction and location before and after the phantom. This task of finding the "Most Likely Path (MLP)" has been developed early on [4] and is now part of the reconstruction procedure. The MLP formalism has been confirmed in beam tests using a subdivided phantom and it was shown that the path inside a phantom can be predicted with sub-mm precision using tracking detectors with ~ 80μm resolution [5].

The requirement that every proton has its MLP reconstructed generates a second challenge: dealing with a large data rate. Tracking and measuring the residual energy of every proton requires fast sensors and fast data acquisition (DAQ). The data flow can be described as follows: assuming 100 protons traversing each $1mm^3$ voxel and using 180 views requires ~ $7*10^8$ protons for a head-size object. With 10 kHz data rate, which is today's norm, one pCT scan will take 20 hrs. A scan with a proton rate of 2 MHz takes 6 min. Such a scan will deliver a dose of 1.5 mGy.

The large number of proton histories and voxels requires the solution of a very large and sparse linear system for image

reconstruction: to reconstruct a 3D image set with 10^7 voxels using 10^9 protons means solving a linear system, Ax = b, with a matrix A of 10^9 rows and 10^7 columns, where b is the vector of integral S.P. along each MLP, derived from energy or residual range measurements, and x is the vector of unknown S.P. values. Solution of such large linear systems requires well known iterative projection methods. Our reconstruction code is currently running on a single general purpose graphics processing unit (GP-GPU) to keep reconstruction times of typical phantom data sets below one hour.

The third challenge of pCT is range/energy straggling. The proton energy loss is not fixed, but is a stochastic process. The straggling uncertainty is a function of depth, irreducible when the energy is not measured. Thus the straggling within the phantom limits the precision of both energy loss and range measurement. A residual range detector will always encounter the maximum range straggling: the range error depends on the energy, and is about 1% of the range (0.1 g/cm^2 at 100 MeV, 0.3 g/cm^2 at 200 MeV), but is independent of the Water Equivalent Path Length (WEPL) of the phantom, since the straggling material in phantom and range counter simply add.

III. Instrumental Choices for pCT Systems

The instrumental challenges of proton radiography and CT are solved by different groups in different ways. This is shown in Table I for a selection of groups involved in proton imaging. For the tracker, the selection includes Gas Electron Multipliers (GEM) [6], Silicon strip detectors SSD [7, 8] and scintillation fibers (SciFi) [9]. There seems to be preference for non-gaseous tracking detectors given the planned use in the hospital environment. For the energy or residual range detector, where the straggling contributes a large fraction of the error, calorimeters [7, 8] and range counters are being used or are under construction [6, 9].

TABLE I. INSTRUMENT CHOICES FOR PCT

Group	Tracker	Energy Detector.	Reference
TERA	GEM	Range+WLSF+SiPM	[6]
Firenze/LNS	SSD	Crystal Cal+PD	[7]
LLU/UCSC/NIU	SSD	CsI+PD	[2], [8]
NIU/FNAL	SciFi+SiPM	Range+WLSF+SiPM	[9]
LLU/UCSC/CSUSB	SSD	Range+Direct SiPM or Polysterene Cal+PMT	(Sect. VII)

Experience with present prototypes and anticipation of use on patients has spawned a new round of upgrades and improvements, which are all designed to address the proton rate issue mentioned in Section II. While at present the proton rate tends to be limited to 10 – 20 kHz, all groups are working on upgrades with data rates in excess of 1 MHz. Consequently, crystal calorimeters are eliminated and replaced by much faster organic scintillator systems, mostly in the form of range counters. There is still diversity in the range counter readout: based on use in HEP, wave length shifting fiber (WLSF) and silicon photomultipliers (SiPM) readout is used, as is direct readout into SiPM or multi-anode PMT. The response of the SiPM readout is somewhat puzzling: in [9], the number of photon electrons (p.e.) in the SciFi signal derived from the 1p.e. noise peak is about 3 times larger than when derived from the width of the signal distribution (Fig. 1). A smaller ratio of 22/13 is found for the range counter signal.

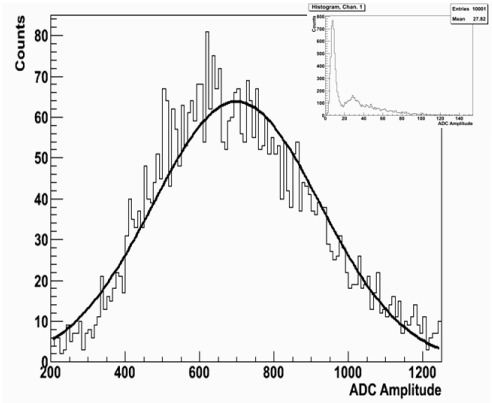

Fig. 1. Pulse height spectrum of 1mm diameter scintillation fibers (SciFi) with SiPM readout for 200 MeV protons [9]. With a 1 p.e. peak at 21 ADC counts, the peak value is estimated at 33 p.e., while relating the width of the signal curve to the number of photo electrons, one gets 9 p.e..

IV. WEPL Calibration

An important step in the reconstruction of pCT images is the derivation of the Water-Equivalent Path Length (WEPL) of each proton in the phantom from energy loss or range measurements. This requires a careful calibration of the instrument in terms the WEPL [8]. This procedure allows the measured signal from the energy or range detector to be converted directly to WEPL and it gives an estimate of the uncertainty of the WEPL measurement. The procedure, which has been developed and tested for the calorimeter of the current pCT prototype, is simple: the phantom is replaced by a set of layers of polystyrene, and the response in the calorimeter is measured. The calibration takes into account the energy loss in all parts of the scanner external to the phantom (Fig. 2): beam pipe window, scattering foil, and tracker planes.

From the RMS of the calorimeter response and the calibration curve WEPL vs. calorimeter response, the errors of the WEPL measurement using the CsI calorimeter can be determined. This is shown in Fig. 5 below.

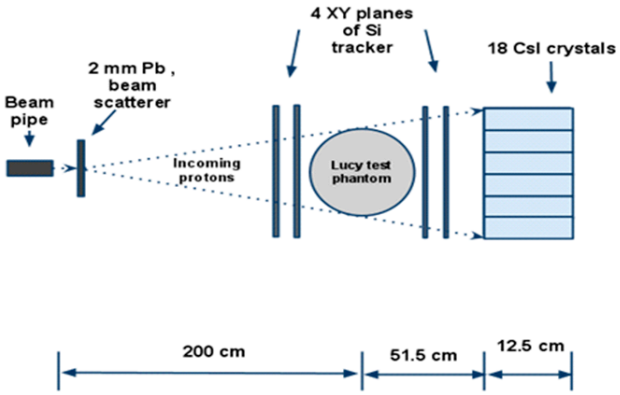

Fig. 2. Schematic set-up of the LLU-UCSC-NIU prototype scanner (not to scale). The position and direction of the proton before and after the phantom are determined with the silicon tracker, and the residual proton energy is measured in the CsI hodoscopic calorimeter.

V. PCT IMAGE RECONSTRUCTION

The proton CT image reconstruction makes use of the WEPL calibration. Before the reconstruction ensues, quality cuts on the calorimeter data are applied and instrumental effects, like the overlap of the silicon detectors and gain difference and position dependence in individual calorimeter crystals are corrected for. The large linear system for pCT reconstruction (see Section II) is best solved with iterative projection methods, for which parallelizable algorithms are readily available It has been shown that it is advantageous, in terms of better final image quality, to choose the reconstruction obtained with the Feldkamp-Davis-Kress 3D modification of the filtered back projection (FBP) algorithm as the zeroth solution, which is then refined, usually in 4-10 iterative cycles through the entire set of linear equations. The FBP method requires re-binning of the data onto a regular spatial and angular grid, while the construction of the linear system for the final reconstruction requires calculation of the proton paths using the MLP formalism (see Section II). Details of the pCT reconstruction development are found in [10]. Fig. 3 shows the reconstructed 2.5 mm slice of a special polystyrene phantom (Lucy, Standard Imaging) with 0.65 mm pixel size. The result of the reconstruction and determination of the relative stopping power RSP is shown in Table II, showing very good agreement between the RSP expected from the NIST data base [11] and the reconstructed RSP from the measurements.

We accumulated data for this reconstructed image during 4 hours at 20 kHz trigger rate (limited mainly by the slow calorimeter and the limited readout rate of the tracker). Such a long scanning time would not be acceptable in clinical applications, and the next development step is a 50 times faster pCT scanner.

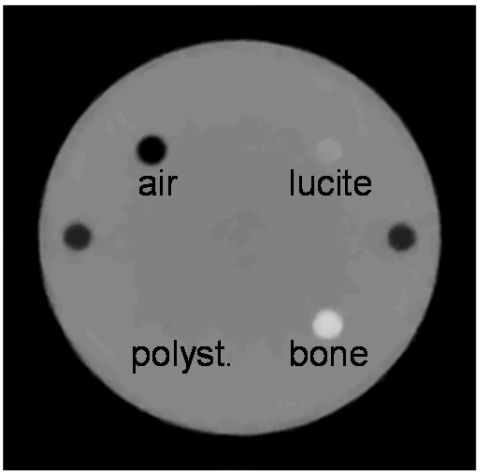

Fig. 3. Reconstructed pCT image of the Polystyrene Lucy phantom (2.5 mm slice, 0.65 mm^2 pixels). The phantom is 14 cm in diameter and contains four cylindrical inserts of 1 cm diameter and 2.5 cm length.

TABLE II. PREDICTED / RECONSTRUCTED RELATIVE STOPPING POWER RSP

Material	Predicted RSP	Reconstructed RSP
Polystyrene	1.037	1.035
Bone	1.70	1.68
Lucite	1.20	1.19
Air	0.004	0.05

VI. DETECTOR SIMULATIONS WITH GEANT4

For a high-speed upgrade of the proto-type scanner, a Geant4 simulation was conducted incorporating all details shown in Fig. 2, but with different calorimeter choices. In the following, a few of the results are listed.

A. Removal of Protons

The main interaction of low-energy protons with matter is ionization described by the Bethe-Bloch equation. But in addition, protons undergo inelastic nuclear interactions, which lead to much larger energy loss per event, compared to electronic interactions. In the response spectra of the pCT calorimeter, protons that have "survived" these inelastic events and are exiting the phantom are moved from the quasi-Gaussian peak into long low-energy tails. Fig. 4 shows both experimental data taken directly from the measured CsI spectra of the WEPL calibration, and Geant4 data from range counter simulations with 1 mm plates. For 200 MeV, between 50% and 70% of the protons will fall into the endpoint peak of the spectra and can easily be used for the WEPL determination. A modeling of the complete spectrum would allow making use of even the events in the tails.

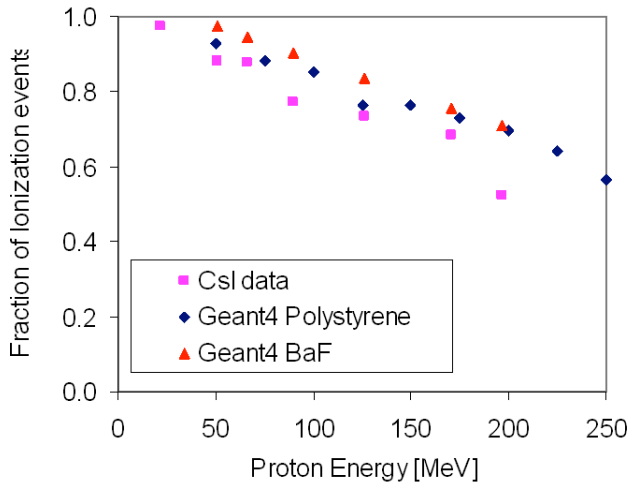

Fig. 4. Fraction of ionization events not affected by inelastic interactions vs. proton energy. This fraction of events lies in the quasi-Gaussian endpoint of the energy spectrum and can be used in the WEPL determination.

B. *Range Detector Resolution*

For range detectors, the thickness of the plates is of special interest. As mentioned above, the resolution is limited by the range straggling in both the phantom and the range detector, which for 200 MeV protons is of the order 3.5 mm. Since the RMS due to the plate thickness is equal to the thickness/√12, somewhat thicker plates will still give close to the same resolution, but with better signal-to-noise ratio and lower channel number. Fig. 5 shows the WEPL resolution from 4 mm plates as a function of WEPL, and the expected constant resolution is evident. In addition, the observed 4 mm WEPL resolution is only 15% larger than the above mentioned minimum value from straggling alone, indicating that plates of ~4 mm thickness are viable for 200 MeV protons. As seen from Fig. 5, the range detector is superior for small WEPL (high proton energy), while at large WEPL (low proton energy) the CsI calorimeter is superior, reaching 1% WEPL resolution.

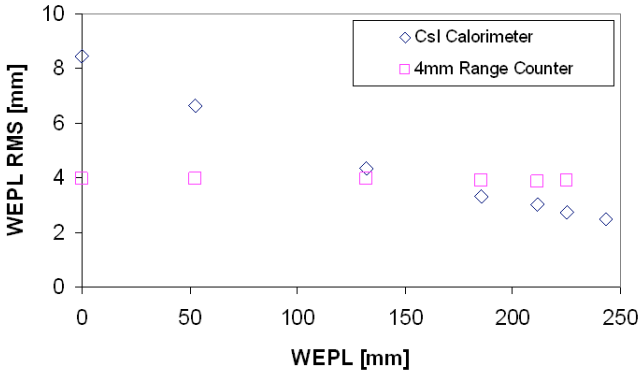

Fig. 5. Error of the WEPL measurement as a function of WEPL, measured for the CsI calorimeter and simulated for a range counter with 4 mm thick polystyrene plates. The expected range counter resolution due to the plate thickness is 1.1 mm.

C. *Tracker Issues*

The main issue for the tracker is the thickness of the silicon sensors. For the thickness of the sensor varying from 200 μm to 400 μm, we find no problem to correct for the finite energy loss in the sensor, which is taken care of by the WEPL calibration anyway. Fluctuations in energy deposited in the Si detector are small compared to the energy straggling in the phantom.

This is true for non-overlapping single sensor planes. When Si sensors are overlapping to cover their dead area like in the present prototype scanner described in Sections IV and V, the variation in effective sensor thickness leads to artifacts in the reconstructed images, if not taken into account properly.

VII. Detector Development for the New PCT Scanner

A. *Data Flow*

As mention before, increasing the data rate to exceed 1 MHz has to be a part of any upgrade toward clinical application. Si sensors are intrinsically fast, so the solution is to build a faster readout ASIC and distributed data acquisition (DAQ), employing local FPGAs for data collection, formatting and transmission.

B. *Energy /Residual Range Detector*

To improve the speed of the energy / residual range detector, the CsI calorimeter of the present prototype is being replaced by a detector based on fast plastic scintillators, and both range counter and calorimeter are under test. A polystyrene range counter with 4 mm plates and direct SiPM readout looks very promising, since preliminary measurements have shown three times the number of photons compared to the WLSF +SiPM readout. In addition, the Geant4 results on range counter with thicker tiles mentioned above are intriguing, and experimental evaluation is pending.

C. *Tracking Detectors*

Silicon strip sensors are attractive since they have low noise at good efficiency, an important factor in a sparse system (no redundant space points). The problem is that their wafer sizes are limited to 6" and that they come with a 1 mm wide dead edge area, which prevents seamless tiling. We are developing "slim edges" on Si sensors which will allow tiling without overlap [12]. This is done in collaboration with the US Naval Research Lab (NRL). Slim edges can be fabricated on finished sensors by a post-treatment involving Laser + XeF_2 scribing, followed by cleaving and PECVD passivation of the edge with nitrogen for n-type and Alumina for p-type sensors. Pictures of the uncut detector and two different slim edges are shown in Fig. 6.

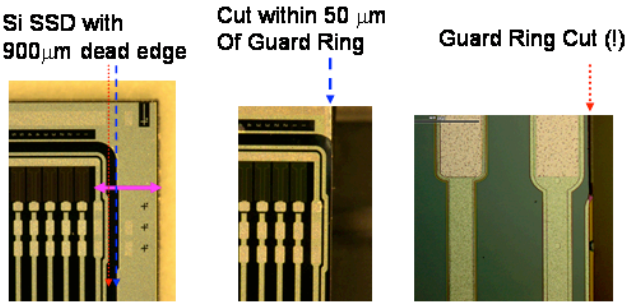

Fig. 6. Edge of a p-on-n HPK GLAST2000 sensors (228 μm pitch). From the left: untreated sensor, sensor with edge close to, but outside the guard ring, sensor with guard ring cut.

Fig. 7 shows the total detector currents for the two slim edge sensors of Fig. 6. They have excellent breakdown behavior. In addition, we have found the charge collection on the strips next to the slim edge to be unchanged when compared to before cleaving. Our process permits reducing the dead edge from 1 mm to < 200 μm.

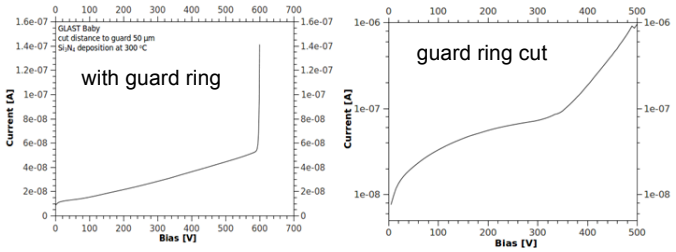

Fig. 7. Total detector currents for the two slim edge sensors of Fig. 6. At 150V bias, the currents are ~10 nA/cm with guard ring, and ~100 nA/cm without guard ring.

VIII. Conclusions

Proton CT has come a long way since our first presentation at the 2002 IEEE NSS-MIC Symposium in Norfolk, VA [1].

We see very different approaches on instruments, motivated in part by a technology transfer from HEP. This has come with severe limitations (like the unacceptably low proton rate).

With the current pCT prototype, we are beginning to see 3D tomographic reconstructions, as well as 2D proton projection radiographs, of acceptable image quality, which will likely improve with further development of 3D reconstruction and 2D projection algorithms.

We are now arriving at a new phase in pCT with dedicated detector development, focusing on large-area edge-less or "slim-edge" tracking sensors and speeding up the data taking to be useful in clinical applications.

End-to-end simulation of the instrument has been essential for our understanding of the requirements and proper choice of the technical solution, yet many additional lessons were learned during experimental operation of the individual detectors and the integrated instrument.

The next crucial step will be technology transfer into a hospital environment and development of clinical testing protocols.

Acknowledgment

Ongoing and unwavering support by Prof. James M. Slater (LLUMC) made this project possible.

The project described was supported by Award Number R01EB013118 from the National Institute of Biomedical Imaging And Bioengineering (NIBIB). The content is solely the responsibility of the authors and does not necessarily represent the official views of the National Institute of Biomedical Imaging And Bioengineering or the National Institutes of Health.

References

[1] H. F.-W. Sadrozinski; V. Bashkirov, B. Keeney, L.R. Johnson, S.G. Peggs, G. Ross, T. Satogata, R.W.M.Schulte, A. Seiden, K. Shanazi, D.C. Williams, "Toward Proton Computed Tomography", *IEEE Trans. Nucl. Sci.,* vol 51, pp. 3 – 9, 2004.

[2] R. Schulte,V. Bashkirov, T. Li; J.Z. Liang, K. Mueller, J. Heimann, L.R. Johnson, B. Keeney, H. F.-W. Sadrozinski, et al. "Conceptional design of a proton computed tomography system for applications in proton radiation therapy", *IEEE Trans. Nucl. Sci.,* vol 51, pp. 866 - 872, 2004.

[3] U. Schneider U., "Proton radiography as a tool for quality control in proton therapy," Med Phys. 22, 353 (1994).

[4] D. C. Williams, "The most likely path of an energetic charged particle through a uniform medium". Phys. Med. Biol. 49 (2004) 2899–2911.

[5] M. Bruzzi; N. Blumenkrantz; J. Feldt; J. Heimann; H. F.-W. Sadrozinski et al., "Prototype Tracking Studies for Proton CT", *IEEE Trans. Nucl. Sci.*, vol 54, 140, 2007.

[6] U. Amaldi et al., "Construction, test and operation of a proton range radiography system" Nucl. Instr. Meth. A629 (2011) pp 337-344.

[7] V. Sipala et al., "Tomographic Images by Proton Computed Tomogrphy System for Proton Therapy Applications", 2011 IEEE/MIC Conference Poster MIC15.S-305.

[8] R. F. Hurley, R. W. Schulte, V. A. Bashkirov, A. J. Wroe, A. Ghebredemin, H. F.-W. Sadrozinski, V. Rykalin, G. Coutrakon, P. Koss, and B. Patyal, "Water-Equivalent Path Length Calibration of a Prototype Proton CT Scanner", submitted. to Medical Physics 2011.

[9] V. Rykalin, private communication.

[10] S. Penfold, "Image Reconstruction and Monte Carlo Simulations in the Development of Proton Computed Tomography for Applications in Proton Radiation Therapy" PhD thesis Univ. of Wollongong, 2010

[11] NIST Pstar: http://physics.nist.gov/PhysRefData/Star/Text/PSTAR.html

[12] V. Fadeyev, H. F.-W. Sadrozinski, J. G. Wright, M. Christophersen, B. F. Phlips, "Performance of P-Type Silicon Sensors after Cleaving and Al2O3 Sidewall Passivation", 2011 IEEE/MIC Conference talk N7-1.